



## A Statistical Survey of Radiation Belt Electron Dropouts

Zheng Xiang<sup>(1)(2)</sup>, Weichao Tu<sup>(2)</sup>, and Binbin Ni<sup>(1)</sup>

(1) Wuhan University, Wuhan, China, 430072

(2) West Virginia University, Morgantown, WV, USA, 26505

### Abstract

Regarding radiation belt dropouts, no previous statistical study using electron phase space density (PSD) to reveal the real loss. Thus, we conduct a statistical study of radiation belt dropouts. If PSD drops by factor >5 within a period less than 8 hours, we call it a dropout event. Based on 4 years of VAP data, we get the dropout distribution as a function of  $\mu$ , K, and  $L^*$  and the relationship with solar wind parameters and geomagnetic parameters. The results show that high  $L^*$  dropouts cover wider  $\mu$ , K range. The low  $L^*$  dropouts mainly follow the influence regions due to EMIC wave. Few dropouts at low  $\mu$ , K due to injection while there are many dropouts with low  $\mu$ , high K, which is likely due to EMIC waves. Dropouts occurring without EMIC influence are company with stronger solar wind and magnetic activity.

### 1. Introduction

To understand and predict the highly dynamic of energetic electrons in Earth's outer radiation belt, it is critical to investigate the complex balance of various acceleration, transport, and loss processes during geomagnetic storms [Reeves et al., 2003; Tu et al., 2009]. Radiation belt dropout is one of the most dramatic variations in the radiation belt, during which the electron fluxes are observed to drop by several orders of magnitude in just a few hours [e.g., Turner et al., 2012a]. It is now widely accepted that both the mechanism of magnetopause shadowing combined with outward radial diffusion and the mechanism of atmospheric precipitations due to EMIC wave induced pitch angle scattering can contribute to radiation belt dropouts [e.g., Tu et al., 2010; Turner et al., 2012b]. However, it is difficult to analyze the relative contributions of these two mechanisms to the observed dropouts. Recently, using high-quality particle and wave observations by Van Allen Probes, Xiang et al. [2017] shed light on distinguishing the dominant loss mechanism at different  $L^*$  regions. They found the evolution of electron PSD versus  $L^*$  profile and the  $\mu$ , K dependence of electron PSD drops can provide critical and credible clues regarding the mechanisms responsible for electron losses at different  $L^*$  over the outer radiation belt. In terms of dominant mechanisms, three distinct radiation belt dropout events studied by Xiang et al. [2017] can be classified into three types in terms of dominant mechanisms: magnetopause

shadowing dominant, EMIC wave scattering dominant, and combination of both mechanisms. The fact that each of these radiation belt dropout events can be classified in terms of different dominant mechanisms immediately leads to an interesting science question: statistically, what is the percentage of each type of dominant loss mechanisms and how do the various solar wind or geomagnetic conditions control the types of dominant loss mechanisms? Therefore, in the present paper, we conduct a comprehensive study of the statistical features of radiation belt dropout events at different  $L^*$  observed by Van Allen Probes from September 2012 to September 2016, namely 4-year time period.

Some previous works have investigated the statistical features of radiation belt dropouts based on the electron flux measurement. Applying superposed epoch analysis to relativistic electron fluxes measured by SAMPEX, Yuan and Zong [2013] showed that statistically high solar wind dynamic pressure leads to larger electron flux dropouts than low dynamic pressure and that southward interplanetary magnetic field (IMF) results in stronger flux decreases compared with northward IMF. A following study of Hietala et al. [2014] adopted the method of normalized superposed epoch analysis to find that interplanetary coronal mass ejection (ICME)-driven sheaths typically produce more than an order of magnitude decrease in the relativistic electron fluxes and that the fluxes can stay below the pre-event level for > 2 days after the sheath passage, resulting from enhanced radial diffusion under magnetospheric compression conditions. However, the decay of electron flux is a mix of real loss and adiabatic variation which can be removed by transferring electron flux to electron PSD as a function of the three adiabatic invariants ( $\mu$ , K, and  $L^*$ ). Shprits et al. [2012] and Ni et al. [2013], using data-assimilative reconstruction of the radiation belt dynamics from multiple spacecraft for statistical analyses, found that 81% of the electron phase space density dropouts are related to moderate increase or sudden jump in the solar wind dynamic pressure and that 68% of identified solar wind dynamic pressure pulses correspond to electron phase space density dropout events. Although, the pitch angle distribution of electron flux from some satellites is assumed rather than directly observed by instruments.

Van Allen Probes particle measurements provide an unprecedented opportunity for statistically evaluating

radiation belt dropout properties due to the availability of electron PSD calculated by electron flux with wide energy and pitch angle coverage together with extensive spatial coverage over the entire inner magnetosphere ( $L < 6$ ) near the equatorial region. Therefore, Van Allen Probes wave data are ideally suited to provide significantly improved statistical results of radiation belt dropout distribution and extent.

## 2. Data and Method

The long term, high quality electron flux with wide energy and pitch angle coverage observed by Van Allen Probes are used to conduct this study. The NASA Van Allen Probes were launched in August 2012 in a highly elliptical and low inclination orbit. These electron flux had been used to investigate distinct dropout events with different dominant loss mechanisms. The observed directional differential electron fluxes during September 2014 to September 2016 are used to calculate the electron PSD as a function of the three adiabatic invariants in the Tsyganenko 04 storm time model (TS04) to remove the adiabatic variations and reveal the real electron loss during the dropout.

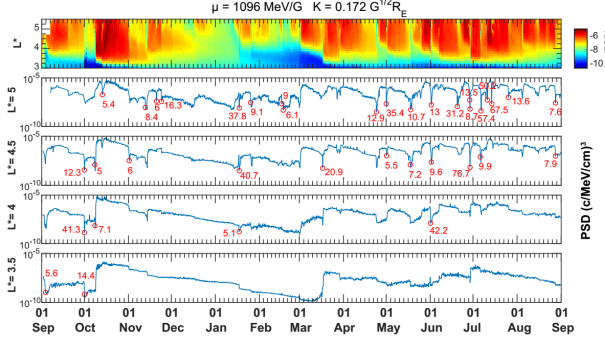


**Figure 1.** Evolution of electron PSD for different  $L^*$  at  $\mu=1096 \text{ MeV}/\text{G}$  and  $K=0.172 \text{ G}^{1/2}\text{R}_E$ .

If PSD drops by a factor  $>5$  within a period less than 8 hours, we call it a dropout event (2 bins). We can see from figure 1 that, in terms of PSD, our radiation belt is also highly dynamic. Prompt dropout is the main influence factor of outer radiation belt rather than slow decay. There are more dropout events occurring at high  $L^*$  regions. However, the higher  $L^*$  dropouts don't always have high drop ratio.

## 3. Results

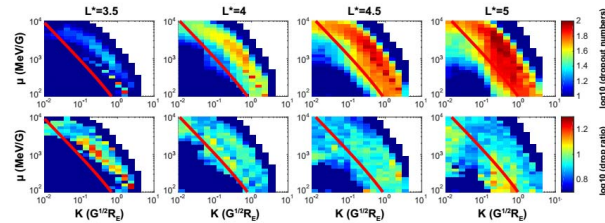


**Figure 2.** Evolution of electron PSD for different  $L^*$  at  $\mu=1096 \text{ MeV}/\text{G}$  and  $K=0.172 \text{ G}^{1/2}\text{R}_E$ . Dropout numbers

and average drop ratio as a function of  $\mu$  and  $K$  at different  $L^*$ .

The red line is electron's lowest resonance energy due to EMIC wave, which means that the part above red can be influenced by EMIC waves. As  $L^*$  increases, red line shift to right, which means less region in  $(\mu, K)$  domain can be influenced by EMIC wave. This is opposite to the intuition that EMIC wave scattering features in energy and pitch angle domain. Same as figure 1, more dropouts occur at high  $L^*$ , during which many are below red line, which is likely due to magnetopause shadowing. There are few dropouts in both low  $\mu$  and low  $K$  regions due to injection. At low  $L^*$ , the  $(\mu, K)$  values with more dropouts follow the red line, indicating EMIC waves play important role in low  $L^*$  region. At high  $L^*$ , low  $K$ , low  $\mu$  dropouts have stronger drop ratio, seems due to the  $\mu, K$  dependence of  $D_{LL}$ . Different previous understanding, there are many dropouts at low  $\mu$ , high  $K$  regions.

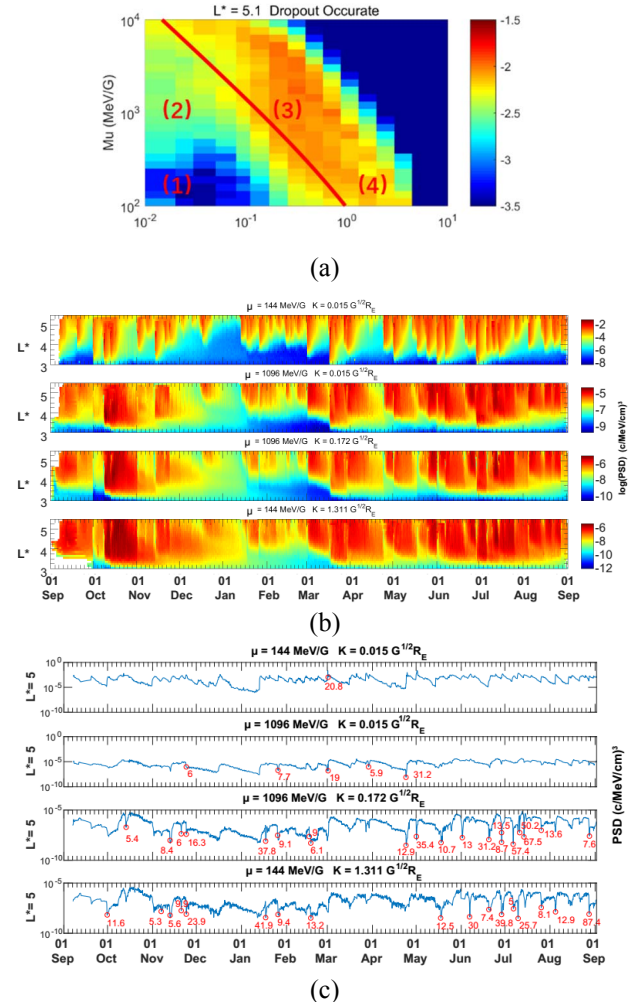


**Figure 3.** (a) Four typical regions to investigate deeply. (b) 1 year of PSD data from VAP at the four  $(\mu, K)$  pairs. (c) 1 year of PSD data at  $L^*=5$ .

We can see regime 1 is mainly influenced by injection or fast convection and then fast decay, probably due to hiss waves. But the other 3 regions decays much slower but suffer from abrupt dropouts. PSD with higher  $K$  have

higher  $D_{LL}$ , leading to more decrease. The dynamics of PSD with low  $\mu$  and high  $K$  is more similar to PSD with higher  $\mu$ .

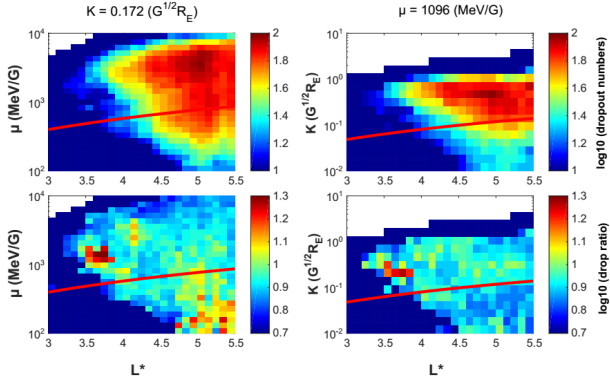


**Figure 4.** Dropout numbers distribution as a function of  $\mu$  and  $L^*$ (left), as a function of  $K$  and  $L^*$  (right).

In the dropout numbers distribution as a function of  $\mu$  and  $L^*$  figure, more dropouts above red line. Dropouts above red line have wider  $L^*$  range. At  $L^* > 4.5$  region, dropouts with low  $\mu$  experience more loss while around  $L^* = 4$  regions, dropouts with high  $\mu$  show more loss. In the dropout numbers distribution as a function of  $K$  and  $L^*$  figure, dropouts above the red line have more numbers and loss.

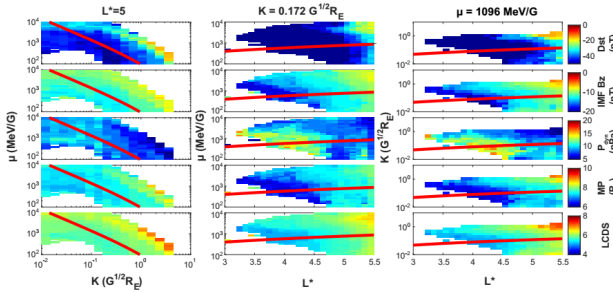


**Figure 5.** Solar wind parameters as a function of  $\mu$  and  $K$  at  $L^* = 5$ , as a function of  $K$  and  $L^*$  at  $K = 0.172 G^{1/2} R_E$ , and as a function of  $K$  and  $L^*$  at  $\mu = 1096 \text{ MeV/G}$ .

At  $L^* = 5$ , dropouts below the red line are company with stronger solar wind activity. At low  $L^*$ , dropouts near red line are company with stronger solar wind activity than dropouts above red line.

## 4. Conclusion

1. High  $L^*$  dropouts cover wider  $\mu$  and  $K$  range;
2. Low  $L^*$  dropouts are more likely to happen above red line;
3. Few dropouts at low  $\mu, K$  due to injection while there are many dropouts with low  $\mu$  high  $K$ , which seems due to EMIC waves;
4. Dropouts under red line show more decrease due to  $\mu, k$  dependence of  $D_{LL}$ ;
5. Dropouts below red line are company with stronger solar wind and magnetic activity.

## 5. Acknowledgements

ECT data were obtained from [https://www.rbsp-ect.lanl.gov/data\\_pub/](https://www.rbsp-ect.lanl.gov/data_pub/), and the solar wind parameters and geomagnetic activity indices were obtained from the NASA OMNIWeb (<http://cdaweb.gsfc.nasa.gov>). LANLGeoMag is downloadable at <https://github.com/drsteve/LANLGeoMag>.

## 6. References

1. H. E. Hietala, K. J. Kilpua, D. L. Turner, and V. Angelopoulos, "Depleting effects of ICME-driven sheath regions on the outer electron radiation belt", *Geophysical Research Letters*, **41**, 7, July 2014, pp. 2258-2265, doi: 10.1002/2014GL059551.
2. B. Ni, Y. Y. Shprits, R. Friedel, R. M. Thorne, M. Daae, and Y. Chen, "Responses of Earth's radiation belts to solar wind dynamic pressure variations in 2002 analyzed using multi-satellite data and Kalman filtering", *Journal of Geophysical Research Space Physics*, **118**, 7, July 2013, pp. 4400-4414, doi: 10.1002/jgra.50437.
3. G. D. Reeves, K. L. McAdams, R. H. W. Friedel, and T. P. O'Brien, "Acceleration and loss of relativistic electrons during geomagnetic storms", *Geophysical Research Letters*, **30**, 10, May 2003, pp. 1149-1164, doi: 10.1029/2002GL016513, 10.
4. Y. Y. Shprits, M. Daae, and B. Ni, "Statistical analysis of phase space density buildups and dropouts", *Journal of Geophysical Research Space Physics*, **117**, January 2012, pp. A01219, doi: 10.1029/2011JA016939.
5. W. Tu, X. Li, Y. Chen, G. D. Reeves, and M. Temerin, "Storm-dependent radiation belt electron dynamics", *Journal of Geophysical Research Space Physics*, **114**, February 2009, pp. A02217, doi: 10.1029/2008JA013480
6. W. Tu, R. Selesnick, X. Li, and M. Looper, "Quantification of the precipitation loss of radiation belt electrons observed by SAMPEX", *Journal of Geophysical Research Space Physics*, **115**, July 2010, pp. A07210, doi: 10.1029/2009JA014949.
7. D. L. Turner, S. K. Morley, Y. Miyoshi, B. Ni, and C.-L. Huang, "Outer Radiation Belt flux Dropouts: Current Understanding and Unresolved Questions", *Geophysical Monograph Series*, vol. 199, edited by D. Summers, I. R. Mann, and D. N. Baker, **199**, 2012, pp. 195-212, doi: 10.1029/2012GM001310.
8. D. L. Turner, Y. Shprits, M. Hartinger, and V. Angelopoulos (2012b), Explaining sudden losses of outer radiation belt electrons during geomagnetic storms, *Nature Physics*, **8**, 8, August 2012, pp. 202-212, doi: 10.1038/nphys2185.
9. Z. Xiang, W. Tu, X. Li, B. Ni, S. K. Morley, and D. N. Baker, "Understanding the mechanisms of radiation belt

dropouts observed by Van Allen Probes.”, Journal of Geophysical Research: Space Physics, **122**, November 2017, pp. doi: 10.1002/2017JA024487

10. C. Yuan, and Q. Zong, “Relativistic electron flux dropout in the outer radiation belt under different solar wind conditions”, Journal of Geophysical Research: Space Physics, **118**, 12, December 2013, pp. 7545-7556, doi:10.1002/2013JA019066.